

THE APPLICATION OF FAD IN THE ASSESSMENT OF ENVIRONMENTAL ASSISTED CRACKING AND FRACTURE CONDITIONS

J.A. Alvarez Laso and F. Gutiérrez-Solana

Departamento de Ciencia e Ingeniería del Terreno y de los Materiales
E.T.S. de Ingenieros de Caminos, Canales y Puertos. Universidad de Cantabria
Avenida de Los Castros s/n, 39005. Santander, SPAIN

ABSTRACT

The environmental working conditions of structural steels, as in the cases of energy and oil installations, established the need to find appropriated methodologies for characterising their cracking resistance. The characterization of very tough steels actually used has been resolved after a methodology that determines the kinetics of cracking as a function of the parameters which control this process, both in elastic and elasto-plastic domains. These parameters unable the crack propagation process to be modelled on a microstructural scale, to be subcritical, either intergranular or transgranular, or critical once final fracture appears.

The application to such modellisation to the structural scale is the objective of this paper. Therefore a FAD (Failure Assessment Diagram) type analysis has been done to define the hydrogen assisted cracking processes in samples of two different microalloyed steels.

INTRODUCTION AND OBJECTIVES

The steels used in piping systems and structural components, such as those in petroleum installations or off-shore platforms, have been continually evolving over recent years. This evolution has been aimed at improving the following characteristics: their mechanical behaviour in order to reduce the amount of material used to optimise transport conditions; their toughness to avoid problems caused by brittle fracture in aggressive working environments and temperatures; their resistance to deterioration, including subcritical cracking processes due to fatigue and/or environment; their workability, guaranteeing good weldability for placement; and their cost. Due to the enormous amount of material necessary for fabricating these installations, the increasing demands made on the steels have been accompanied by steadily increasing minimum performance qualities to guarantee safe working conditions [1].

Under working conditions such as in off-shore platforms these steels are subjected to stress corrosion cracking (SCC) problems in marine environments associated with situations involving cathodic protection or sulfide induced cracking due to bacterial activity [2]. In both cases hydrogen plays a fundamental role in the cracking mechanisms and therefore these steels should be shown to be resistant to HIC. Under those conditions the subcritical propagation processes which involve both type, intergranular and cleavage transgranular, can be present in conjunction with other critical processes like microvoids. Due this, the conventional characterization methods are not useful. In previous works a new methodology was developed in order to characterize the SCC behaviour of steels showing a high resistance to subcritical propagation processes [3-4]. The objective of the present work is to thoroughly improve this methodology by means of a new develop which make possible the direct application to design of structures by means of FAD.

Fault Diagrams are, in this respect, a tool which has been widely used in the evaluation of structural safety, with highly satisfactory results. These diagrams, in their classical form, take in two main areas: one of reliable design and the other of unreliable design, this being considered as the possibility of fracture through plastification or through unstable crack propagation, or a combination of both. This representative structure

does not, however, take into account the possibility of subcritical propagation, that is, that which does not lead to the fracture or collapse of the structure immediately.

There is, then, a need for the definition of a new type of representation for the use of FAD in the design of HIC phenomena. Although the classical form of the critical fracture produced by the instability in the crack propagation is still applicable in many cases, it is also necessary to reflect the non-unstable propagation processes present in HIC processes. In the classical representation, such processes would remain within the safety zone.

MATERIALS AND CONVENTIONAL CHARACTERIZATION

The materials to be characterized are two microalloyed steels taken from industrial heats. Their chemical composition is presented in Table 1. The first steel, E690, has a high yield strength and is used in the manufacture of self-elevating lift belts for oil platforms. The second, E500, is a steel with a medium yield strength and is used in the manufacture of semi-tubular stabilizers for the above-mentioned lift belts to which they are welded. Both steels are subjected to water quenching, later tempered at 600°C (E690) or 650°C (E500), and finally air cooled. These treatments lead to a tempered bainite microstructure in both steels.

The results of the mechanical characterization performed on both steels using tensile tests are summed up in Table 2. The fractographic study performed on the fracture surface of the tested tensile strength samples shows that in both steels fracture occurs because of microvoid coalescence. The toughness of both materials was characterized by determining the *R* curve of the *J* integral following the method proposed by the European Group of Fracture ESIS P1-92 Normalised 25 mm thick compact CT specimens were machined from the available material. Tests were performed on each material at two loading rates under displacement control, v_d , at $4.1 \cdot 10^{-6}$ and $4.1 \cdot 10^{-7}$ m/s. The results show that the materials possess a high toughness which is independent of loading rate. The toughness is much higher in the E500 steel for which $J_{0.2/BL}$ reaches a value of 1017 kJ/m² compared with 259 for the E690 steel.

TABLE 1
CHEMICAL COMPOSITION OF STEELS E690 AND E500 (% BY WEIGHT)

Steel	C	Si	Mn	Ni	Cr	Mo	Cu	Sn	Al	V	Ti
E500	0.063	0.23	1.36	0.585	0.115	0.195	0.103	0.003	0.017	0.048	<0.003
E690	0.135	0.241	1.1	1.518	0.496	0.465	0.18	0.009	0.078	<0.003	0.003

TABLE 2
CHARACTERISTIC TENSILE PARAMETERS OF THE DIFFERENT MATERIALS

Steel	E500	E690
s_y (MPa)	530	840
s_u (MPa)	640	915
e_{max} (%)	9	6.5

BEHAVIOUR IN HYDROGEN INDUCED CRACKING CONDITIONS

HIC processes were characterized by testing 25 mm thick CT specimens in an aggressive environment at a constant loading rate. The aggressive environment was obtained by cathodic polarization at different current densities in a solution of 1N of H₂SO₄. The samples were subjected to a process of continued polarization for 40 hours before and throughout the mechanical test. Crack propagation occurred at this stage and finally led to the specimen's breakage. A later SEM fractographic study revealed the mechanism behind the cracking process.

By applying a suitable analytical methodology [3-4], based on the EPRI procedure [5] for characterizing the behaviour of cracked components in elastic-plastic regime, at any moment it is possible to know the crack

length values, a , the crack propagation rate, da/dt , and the J integral. Fig. 1a shows the load-displacement behaviour curve for one of the tests and both Figs. 1a and 1b the characterization obtained from it. The equivalent stress intensity factor, K_J , has been determined from the J integral value. The threshold conditions, K_{th} ; the subcritical propagation rate, $(da/dt)_{sc}$; the critical fracture condition initiation value, K_c ; and the critical propagation rate, $(da/dt)_c$, are all defined in Fig. 1b. Tests were performed under different aggressive conditions by varying both the polarising current density and the loading rate. Table 3 presents all the results obtained.

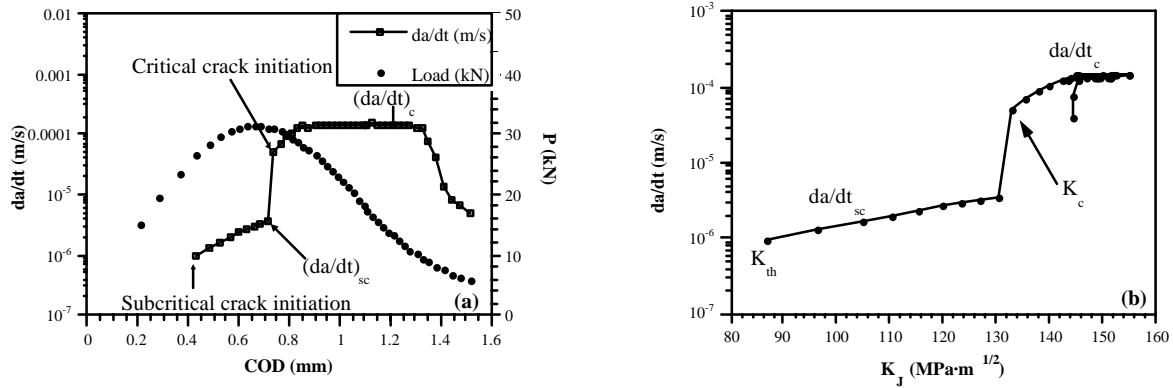


Figure 1: Characterization of the cracking process through the da/dt - K_J (b) curve obtained from the load displacement curve (a)

TABLE 3
CHARACTERISTIC PARAMETERS FOR THE HIC PROCESSES TESTED IN THE TWO STEELS

Steel	Current density (mA/cm ²)	Displacement rate v_d (m/s)	K_{th} (MPa m ^{1/2})	$(da/dt)_{sc}$ (m/s)	K_c (MPa m ^{1/2})	$(da/dt)_c$ (m/s)
E500	5	$4.1 \cdot 10^{-7}$	105	$2 \cdot 10^{-7}$	160	$3 \cdot 10^{-6}$
E500	5	$4.1 \cdot 10^{-8}$	80	$8 \cdot 10^{-8}$	142	$4 \cdot 10^{-7}$
E500	5	$4.1 \cdot 10^{-9}$	68	$2 \cdot 10^{-8}$	123	$1 \cdot 10^{-7}$
E500	5	$8.2 \cdot 10^{-10}$	64	$7 \cdot 10^{-9}$	100	$1 \cdot 10^{-7}$
E690	1	$4.1 \cdot 10^{-8}$	120	$5 \cdot 10^{-8}$	260	$8 \cdot 10^{-8}$
E690	5	$4.1 \cdot 10^{-7}$	87	$4 \cdot 10^{-7}$	132	$5 \cdot 10^{-5}$
E690	5	$4.1 \cdot 10^{-8}$	63	$2 \cdot 10^{-7}$	120	$1 \cdot 10^{-6}$
E690	5	$8.2 \cdot 10^{-10}$	39	$1 \cdot 10^{-7}$	44	$3 \cdot 10^{-6}$

MODELLING

Most models, such as that described in [6], attempt to explain both the fracture mode, whether it be IG or TG, and the parameters of mechanical behaviour in CBT for low-alloy and high elastic limit steels in aggressive aqueous environments, similar to those presented here, in which the presence of hydrogen in the crack head plays a fundamental role [7-16].

In this case, the model establishes that the crack propagation in CBT takes place as a succession of local isolated fractures, nucleated and developed at the crack-base plastic zone. These local fractures nucleate when the plastic strain applied reaches certain critical values determined by the fragilisation produced in this plastic zone by the presence of the hydrogen absorbed by the material, the solubility of the hydrogen being greater in this zone than in the rest of the metallic network. Thus, the model establishes that the crack propagation is controlled by the kinetics of the hydrogen throughout its entrance and diffusion through the crystal network.

This model proposes that the nucleation of local fractures, which produce the crack propagation, takes place in specific defects of the crystal network, as a limit in the martensitic or bainitic laths, occurring close to the grain border or, sometimes, in non-metallic inclusions, constituting traps in which the hydrogen concentration is very high and, consequently, the value of critical strain in its environment is particularly low.

The type of fracture which arises during propagation, IG or TG, is directly associated to the nucleation process described. If the nucleation occurs at the grain border, the fracture will be intergranular, while if it occurs inside the metallic grain, it will be transgranular. This is established through conditions of the relation grain size (d) – position of nucleation (L^*) – size of plastic zone (r_p) which finally lead to limiting expressions for the threshold values of propagation for IG and TG fractures as a function of micro-structural parameters and the mechanics of the material. These conditions transferred to macroscopic parameters, such as K , lead to the following expressions:

IG Condition:

$$\delta_{Isc} < \frac{d}{2.3} \quad \acute{o} \quad K_{Isc} < 0.85 \sqrt{\sigma_y E d} \quad (1)$$

TG Condition:

$$\frac{d}{2.3} < 4\delta_l \Leftrightarrow \delta_l > \frac{d}{9.2} \quad \acute{o} \quad K_{Isc} > 0.42 \sqrt{\sigma E d} \quad (2)$$

These conditions can be applied to P-COD load-shift representations for a given specimen with a constant crack length, of a material with known parameters to define the predictable transgranular or intergranular fracture fields.

The aim of this paper is to verify whether the crack conditions observed in the studied steels in the various environments tested (1,5 and 10 mA/cm²) comply with the modelling presented. To this end, Figures 2 and 3 present simultaneously two situations on the theoretical P-COD curves for CT specimens of 25 mm thickness for both materials with crack lengths varying between 32 and 40 mm:

- a) The real curves for the tests performed in the medium corresponding to different strain speeds, superimposing on these the micro-mechanisms observed: cleavages plus IG and cleavages alone, both subcritical, and critical microholes.
- b) The representation in each case of the maximum limit conditions of intergranularity (1) and the minimum limit of transgranularity (2).

As can be observed in Figure 2, for the E690 steel, the initial mixed subcritical processes of cleavages and intergranularity for all cases are inside the field limited by conditions under which the IG and TG processes may be simultaneous. Moreover, there are no cleavages below condition (2), nor is there any intergranularity above condition (1). All of this is in agreement with the predictions of the model. The same degree of fulfilment can be appreciated for the E500 steel in Figure 3.

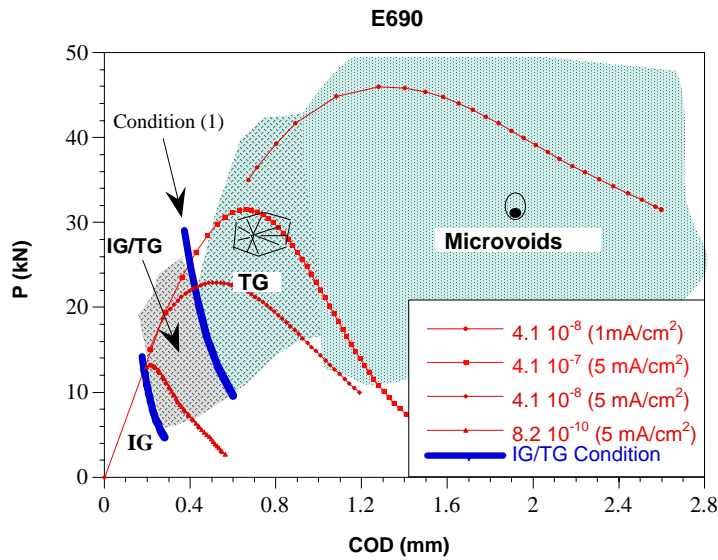


Figure 2: P-COD curves for E690 steel, showing the micro-mechanism zones observed and the IG and TG conditions of the model

Thus, the micro-structural and mechanical conditions which determine the modelling conditions continue to be valid for this material and environmental situation.

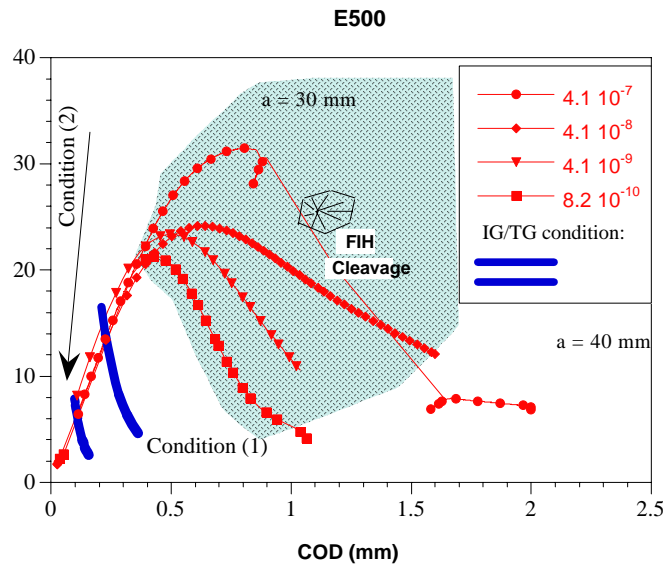


Figure 3: P-COD curves for E690 steel, showing the micro-mechanism curves observed and the IG and TG conditions of the model.

Extension of behaviour model to FIH processes with definition of limit conditions of subcritical processes

The extensive studies carried out in the area of hydrogen induced cracking [17] provide a firm basis for the extension of the model through the establishment of the limit conditions of local strain for which subcritical processes arise under mechanisms without any observable strain, intergranularity or pure cleavage. A distinction is made between those processes which give rise to crack processes with severe tearing as a prolongation of previous processes and those which lead to crack processes through formation and microhole coalescence. These conditions are established on the basis of the fact that the subcritical processes corresponding to low strain situations remain associated to local conditions controlled by values of the J integral for which the elastic component J is the major one, while subcritical situations with tearing

or critical situations are associated to values of the J integral in which the plastic component, J, is significant.

In previous papers [3], it has been shown that the condition of abandonment of the elastic domain zone, defined by the equality

$$J_e = 0.95 \cdot J \quad (3)$$

is produced for each steel studied at a constant shift value, independently of the crack length presented by the specimen. This can be seen in Table 4, with a particularly constant COD for each steel, independently of the crack length, and in Figures 4 and 5 through condition 3

The analysis of what the situation of a constant shift represents on a local level for the initiation of a relevant local plastification has been made for the two steels. In both cases, the situation has been analysed as a function of the crack length, verifying that it can be associated to a constant value in the relative size of the plastic zone at the length of the remaining ligament, $r_y/W-a$. In the E690 steel, this relative value is 1/6, after which there is critical propagation through formation and microhole linking, that is, through a process of local instability, such as that normally corresponding to an instability produced by global plastification.

TABLE 4
DETERMINATION OF CONDITIONS OF FULFILMENT OF EQ.(3) FOR STEELS E500 AND E690

a(mm)	E500		E690	
	COD (mm)	J_e (kJ/m ²)	COD (mm)	J_e (kJ/m ²)
32	0.50	38	0.95	140
36	0.48	27	0.92	100
40	0.52	18	0.94	70

In contrast, for the E500 steel, this value is only 1/12, thus giving rise to mechanisms which bring about an ever-increasing degree of plastic strain, but which offer continuity with the previous subcritical elastic process, which means that the cleavages have increasing degrees of tearing.

Bearing in mind the above observations, the conditions of instability through ligament plastification in their limit value have been obtained for each specimen in plane strain conditions, and are shown in the graphs of Figures 4 and 5, corresponding to steels E690 and E500, respectively.

As can be observed in Figure 4, the low hardening capacity of steel E690 means that the condition of plastic instability in the P-COD field is close enough to that of the initiation of the relevant local plastic conditions, establishing that it passes almost directly from the subcritical process to the critical hole formation processes. In contrast, the E500 steel, due to its greater hardening capacity, shows an important separation between the two limits, so that it presents subcritical and even critical processes with a torn cleavage morphology. Only in the open air test does this steel attain consistently, with its P-COD curve, the local conditions corresponding to hole formation conditions.

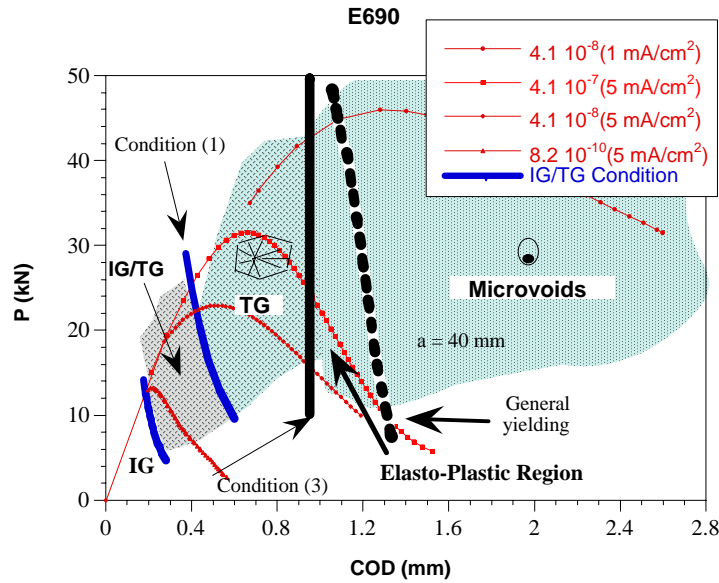


Figure 4: P-COD curves for tests of steel E690 steel, showing the micromechanism zones observed and conditions of end of elastic domain and plastification

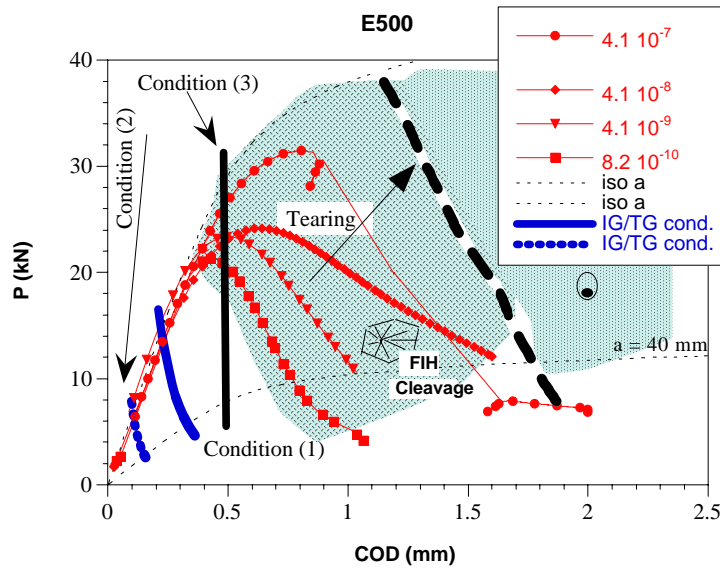


Figure 5: P-COD curves for tests of steel E500 at 5 mA/cm², showing the micromechanism zones observed and conditions of end of elastic domain and plastification

Thus, the limit conditions of subcritical propagation in the intergranularity and transgranularity domains, maxIG and maxTG for each material, together with those of initiation of the relevant plastic strain mechanisms, (3), and the global limit of the subcritical mechanisms, provide a behaviour model for the studied geometry. Figures 6 and 7 show these conditions for the cases studied.

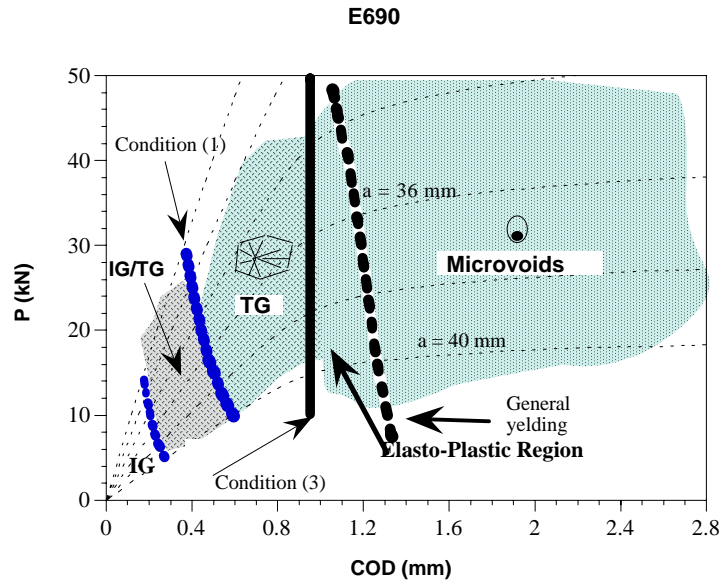


Figure 6: Modelling of the different behaviour zones in FIH processes for the E690 steel

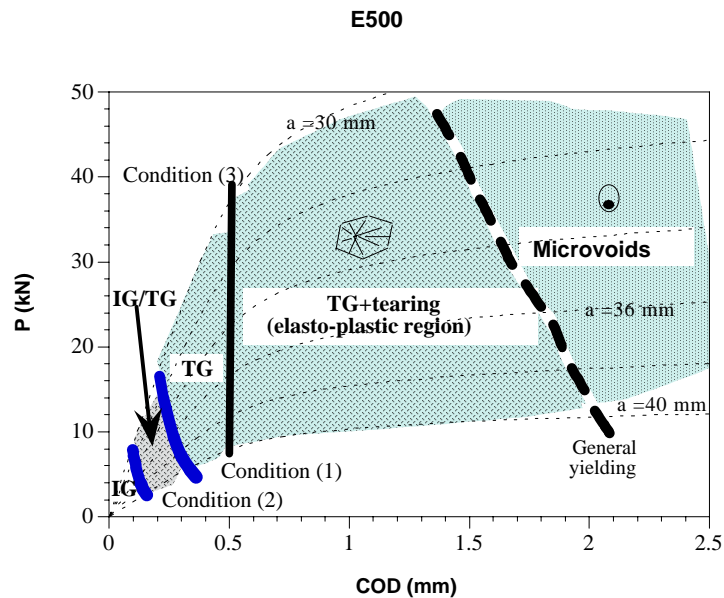


Figure 7: Modelling of the different behaviour zones in FIH processes for the E500 steel

APPLICATION OF FAD IN STEELS E500 AND E690 STEELS

The E500 and E690 steels have been substantially characterised in a wide range of environmental and mechanical strain conditions, producing behaviour models for the HIC conditions described in the first part of this paper.

The application of these models to real components, in this case a compact specimen, defines regions with shared characteristics in their macro-structural behaviour. The representation of these regions in P-COD diagrams is an initial design tool. Figures 6 and 7 show these representations for the steels studied in this paper.

The transfer of the P-COD representation with defined borders for the micro-mechanical models to a FAD diagram constitutes a further step in the unification of design criteria which are firmly rooted in micro-mechanical models and which can, therefore, be applied in any situation.

Figure 8 shows the classical fault diagram defined for steel E500, representing the fault line and the behaviour curves for a compacted specimen with different crack lengths and assuming that no type of propagation is developed. We can thus identify these curves with the iso-a of the P-COD diagram.

The representation of the IGmax and IGmin limits are a function of the stress intensity factor defined in (1) and (2) and must therefore correspond to straight lines parallel to the axis K_r , in the FAD representation. Figures 9 and 10 show these curves for both cases.

The third limit to define is the initiation of instability through tearing, coincident with the development of the plastic component of the J integral (Table 4). This line in the fault diagram corresponds to a representation parallel to the K_r axis, with a L_r value of 0.85 for the E690 steel and at 0.75 for the E500 steel.

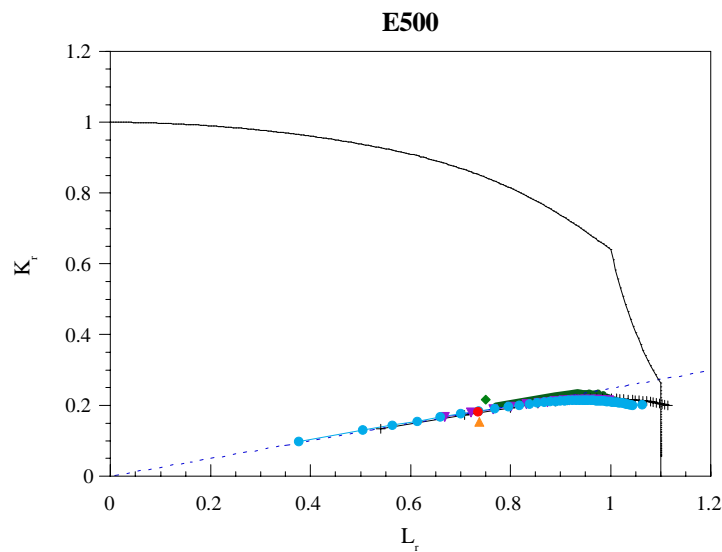


Figure 8: FAD diagram for different conditions on E500 steel

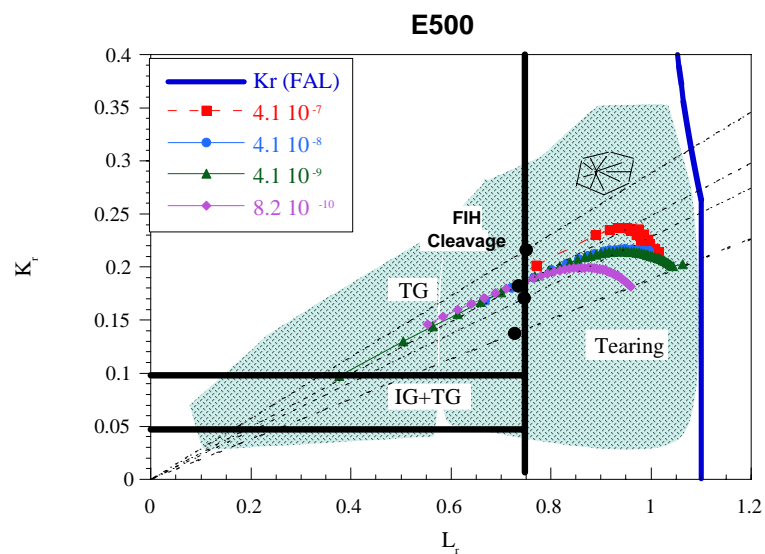


Figure 9: FAD diagram for different conditions on E500 steel, showing micromechanisms of crack propagation

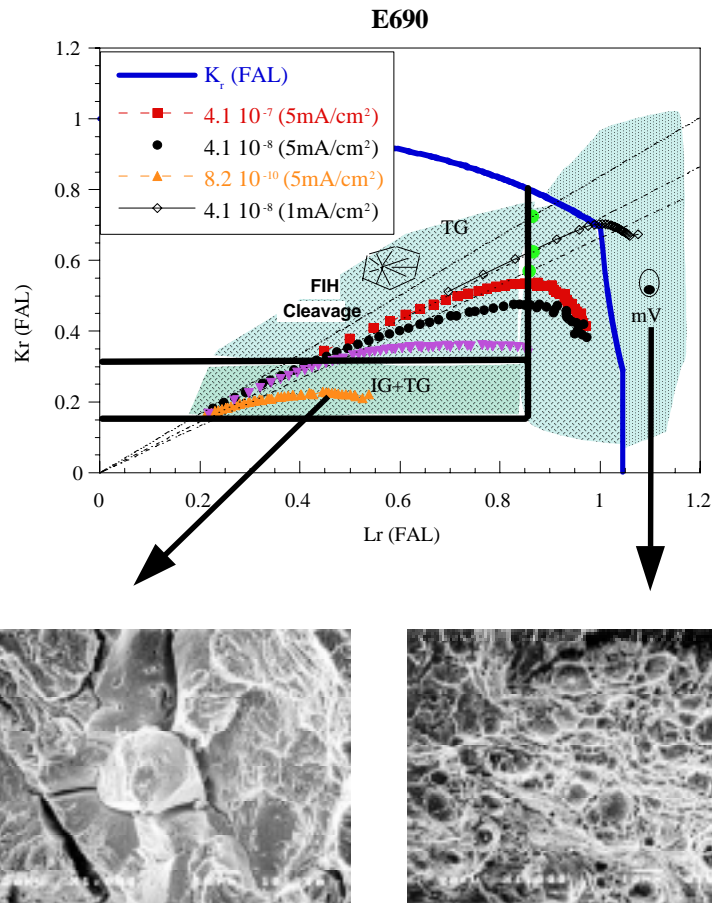


Figure 10: FAD diagram for different conditions on E690 steel, showing micromechanisms of crack propagation.

CONCLUSIONS

The microalloyed steels with a bainitic structure tested have been shown to be susceptible to presenting HIC processes. This susceptibility follows the rules of a classic dependence:

- On material: apparently those with higher yield strengths are more susceptible when the comparison is made using similar microstructures.
- On environmental aggressiveness: as the concentration of hydrogen present in the material grows its susceptibility to cracking increases and this cracking is produced following more brittle mechanisms.
- On loading rate: which affects the materials susceptibility in given environmental conditions, not through changes in the fracture micromechanisms but through the parameters which define the typical cracking conditions and their kinetics.

The combined action of a given stress state and loading rate determine the time which hydrogen is active in the crack tip process zone, provoking different types of cracking: microvoids coalescence, cleavage, or intergranular. Fracture type depends on hydrogen concentration and on the applied stress intensity factor. These two parameters were varied during the tests producing, as has been demonstrated, changes in the type of crack propagation in the same specimen.

Both, the P-COD and FAD has show its capacity to be a useful tool in order to relate the micromechanisms responsible of crack propagation and the design parameters able to be used in structural analysis as can be appreciate in Figure 10.

ACKNOWLEDGEMENTS

This work is part of the ECSC programme 7210-KB/934 funded by the Spanish Interministerial Commission of Science and Technology by the agreement CICYT MAT 93-0970-CE.

REFERENCES

- [1] H. Chino, M. Abe, K. Katayama, H. Takemiro and H. Akazaki: in *Pipeline Technology Conference*, Oostende, Belgium, (1990), Part A, pp. P.4.1.
- [2] G. Gabetta and I. Cole: *Fatigue Fract. Engng. Mater. Struct.*, Vol. 16, No. 6, (1993), pp. 603.
- [3] J. A. Alvarez, *Aplicación de la Mecánica de la Fractura Elastoplástica a Procesos de Corrosión Bajo Tensión*. Doctoral Thesis, University of Cantabria, (1998)
- [4] F. Gutiérrez-Solana, J. A. Alvarez, in *An. Mec. de la Fract.*, Vol. 14, (1997), pp. 50-68
- [5] V. Kumar, M.D. German and C.F. Shih: *An Engineering Approach for Elastic-Plastic Fracture Analysis*, General Electric Company, NP-1931, Research Project 1237-1, Topical Report, Schenectady, New York, (1981).
- [6] Gutiérrez-Solana, F., Valiente, A., González, J. and Varona J.M., "A Strain-Based Fracture Model for Stress Corrosion Cracking of Low-Alloy Steels", *Metallurgical and Materials Transaction A*, Vol. 27A, pp. 291-304 (1996).
- [7] Thompson, A.J. and Bernstein, I.M.; *Advances in Corrosion Science and Technology*, Fontana and Stachle, eds. vol. 7, Plenum, NY, 1980, p. 53.
- [8] Kennedy, J.W. and Whittaker, J.A.; *Corrosion Science*, 1968, vol. 8, p. 359.
- [9] Beachem, C.D.; *Met. Trans.*, 1972, vol. 3, p. 437.
- [10] Louthan, M.R.; Donovan, J.A. and Rawl, D.E.; *Corrosion*, 1973, vol. 29, p. 108.
- [11] Gerberich, W.W.; *Hydrogen in metals*, Bernstein and Thompson, eds., ASM, Metals Park, Ohio, 1974, p. 115.
- [12] Speidel, M.O.; *Hydrogen in metals*, Bernstein and Thompson, eds., ASM, Metals Park, Ohio, 1974, p.575.
- [13] Thompson, A.W. and Bernstein, I.M.; *Rev. Coating Corrosion*, 1975, vol. 2, p. 3.
- [14] Williams, D.P. and Nelson, H.W.; *Met. Trans.*, 1972, vol. 3, p. 2107.
- [15] Speidel, M.O.; "Theory of Stress Corrosion Cracking in Alloys", J.C. Scully, eds., NATO, Bruselas, 1971, p. 289.
- [16] Marsh, P.G. and Gerberich, W.W.; *ISCC, Materials performance and evaluation*, Jones, R.H. de., ASM, Materials Park, 1992, p.63.
- [17] Gutiérrez-Solana, F., Alvarez, J. A., Brass A.M, Chêne, J., Coudreuse, L., Astiz, M.A., Renaudin, J. and González, J.J., "Stress Corrosion Cracking on Weldable Microalloyed Steels" ECSC Contract nº 92.F2 11a 7210, Final Report, April 1996.

Rapid Communications

E-mail address: alvareja@ccaix3.unican.es
gsolana@ccaix3.unican.es

Fax: 34-42-201818

Phone: 34-42-201819